Wear 576-577 (2025) 206143

Contents lists available at ScienceDirect

Wear

journal homepage: www.elsevier.com/locate/wear

Investigation of the chemical structure and antiwear performance of biochar used as a grease additive

Jarosław Molenda [a,*], Monika Makowska [a], Jerzy Kubacki [b], Marcin Sikora [b], Maciej Łuszcz [a], Edyta Osuch-Słomka [a]

[a] Łukasiewicz Research Network – Institute for Sustainable Technologies, Pulaskiego 6/10, 26-600, Radom, Poland
[b] University of Silesia in Katowice, Faculty of Science and Technology, Institute of Physics, 75 Pulku Piechoty 1, 41-500, Chorzow, Poland

ARTICLE INFO

Keywords:
Biochar
Biomass
Grease additive
Friction
Lubrication
Antiwear performance

ABSTRACT

The aim of the work was to investigate the influence of the microstructure of biochar additives on the antiwear performance of lithium greases. The novelty of this work is the investigation of the possibilities of effectively replacing the critical raw material (graphite), used as an anti-wear additive to greases, with biochar derived from agricultural waste and to study the impact of biochar on the friction surface. The initial grease based on paraffin oil and lithium stearate and four greases additionally enriched with 3 wt% or 5 wt% of biochar produced during the pyrolysis of flax or wheat biomass were tested. All the greases had an NLGI grade of 2. The biochar additives were examined using FTIR, and the I_D/I_G ratio was determined based on Raman spectra. Friction tests were carried out in a roller-block system made of 100Cr6 bearing steel. After the tests, the volumetric wear of the blocks was determined using a profilometer and the chemical structure of the friction surfaces was examined using SEM/EDS and XPS. The research has confirmed that a higher content of biochar in the grease reduces the volumetric wear of the blocks more effectively. The best tribological properties were demonstrated by the grease containing 5 wt% of flax biochar, which resulted in a 24 % reduction of wear compared to the wear of the block lubricated with the model grease. It was found that additives with more highly ordered graphite structures (I_D/I_G = 0.33) and without oxygen functional groups showed better antiwear performance than biochar additives containing such groups but with a more disordered structures (I_D/I_G = 0.44). The wear tracks included iron oxides and thin layers of greases that were not removed when the blocks were ultrasonic cleaned after the tests. Further analysis will allow to determine the mechanism of boundary layer formation. Then researchers will be able to present the results in a subsequent paper.

1. Introduction

Friction and wear are the main causes of mechanical device failure and higher energy consumption [1]. Improving the reliability of machines and the efficiency of their work is one of the greatest challenges of the modern world due to the growing concern for the environment. The global friction and wear losses, economic costs, and CO_2 emissions are huge. It is estimated that 103 EJ of energy is currently used to overcome friction. Moreover, 16 EJ is consumed to regenerate worn parts and spare equipment due to wear damage and failures. Worldwide, the total cost of friction and wear is €250,000 million and the total CO_2 emissions amount to 8120 Mt [2]. Experts predict that by 2032 – owing to the implementation of advanced technologies, materials, and lubricants – it will have been possible to reduce energy losses by 40 %, which would bring global savings of 1.4 % of the GDP yearly. It would also result in a global CO_2 emission reduction by up to 3140 Mt and cost savings of €970,000 million [2].

One way to reduce such energy losses is to minimise the friction between moving parts, e.g. by using graphite-based solid lubricants [3 [4] or a suitable lubricant/grease [5,6]. Nowadays, more than 90 % of rolling bearings are lubricated with grease [7]. In grease lubrication, the mechanisms of possible tribofilm formation on sliding surfaces still remain largely unexplored, which is a serious knowledge gap that requires intensive research. However, the liquid lubricant can form a thin layer on the surfaces of friction elements, preventing their direct contact, and thus significantly reducing the coefficient of friction and wear [1]. There is a growing demand for new, improved lubricant formulations. Such lubricants (base oils and additives) should guarantee both

* Corresponding author.
E-mail address: jaroslaw.molenda@itee.lukasiewicz.gov.pl (J. Molenda).

https://doi.org/10.1016/j.wear.2025.206143
Received 20 March 2025; Received in revised form 16 May 2025; Accepted 22 May 2025
Available online 25 May 2025

the best tribological properties and a reduced environmental impact. Mineral-based oil is traditionally used to lubricate sliding elements (its consumption is the largest in the world by volume), although synthetic-based oils are gaining popularity due to their very high thermal and oxidative stability and longer service life. One of the most promising ways to further improve the efficiency of mineral lubricants and greases is to use carbon additives, i.e. graphite and carbon nanostructures (0D, 1D, 2D) [1,2,6–12]. These carbon-based additives provide friction reduction, and the lubricity of the grease depends on the size and distribution of the carbon particles (e.g. graphite) contained therein [13]. In particular, carbon quantum dots and two-dimensional graphene-based nanostructures are increasingly indicated as a potential new generation of lubricant additives. They are characterised by good mechanical, thermal, electrical, and chemical properties, often even at very low concentrations [10 [11]

However, carbon nanostructures are not without drawbacks. A major limitation in their application is the tendency to agglomerate and a relatively poor dispersion stability in the base oil, caused by their high surface energy [8 [11]The solution to this problem may be a chemical or physical modification of carbon additives, but such materials are still in the research phase and are not commonly available in the market [14]. The structure of these additives opens wide functionalisation opportunities towards obtaining not only better dispersibility, but also lubricity and multidirectional action in the lubricants and greases (as multifunctional additives) [11,14]. The functionalisation can be used as a tool to promote or inhibit various lubrication mechanisms. For example, the bonding of long, straight hydrocarbon tails on the surface of graphene oxide ensures good effectiveness of the lubricants as friction modifier and antiwear additives, and improves dispersion stability in the base hydrocarbon oil [14]. On the other hand, the chemical modifications of graphene by hydrogenation, fluorination, or oxidation are not effective and cause increasing in friction [10].

Carbon nanostructures are often treated as biocompatible and non-toxic due to the similarity of their structure to harmless three-dimensional carbon allotropes, such as graphite or diamond [15]. However, there is no sufficient scientific evidence confirming their non-toxicity *in vivo* and *in vitro* [16 [17] Experts still disagree on this matter. At the same time, there are reports about their biocompatibility [18] and toxicity [17 [19,20]There is a risk that the nanoparticles will be released into the environment during their production, transport, consumption, and utilisation, and then they will penetrate through the physiological barriers and cellular structures of organisms [19]. It probably depends on the method of application, exposure time, and concentration, and this calls the current commercial use of carbon nanostructures as lubricant additives into question. This requires caution in their use and further research that will dispel these doubts. However, there are papers [21 [22] on the use of, for example, graphite additives in greases. These additives are devoid of these disadvantages and show high antiwear performance.

The growing emphasis on environmental protection has resulted in the search for new breakthrough lubrication technologies and increased the demand for more environmentally acceptable lubricants (EALs) [11]. There is a great demand for lubricants that are not only more resistant to leakage and exhibit non-dripping and sealing properties, but also have the ability to retain particles of nano- and micrometer-sized additives in suspended form [6,23]. Lubricants that meet the EU Ecolabel criteria have a lower adverse impact on water and soil (biodiversity), their production is characterised by lower CO_2 emissions and they contain renewable raw materials increasingly [24]. In the future, lubrication systems will have to meet progressively more strict regulations and environmental requirements. It will often be necessary to replace existing lubricants with more environmentally friendly ones. In the near future, the following aspects and requirements of a more environmentally friendly lubricant production must be considered and met [11]: availability of raw materials, independency from petroleum or fossil fuel sources, reduction of the CO_2 footprint, new synthesis pathways, and other specific performance requirements for lubricants.

On the other hand, ~700 million tonnes of crops are wasted every year in Europe, and food production and supply chains already consume around ~30 % of the world's total energy production [25,26].

After harvest, the grain is separated from the stalk, leaving straw, or in the case of fibre crop (e.g. flax) – the shives. The demand for straw as animal feed is decreasing, while grain production is increasing. The straw and shives are used as a natural fertiliser. However, the existing oversupply of this type of biomass raw material leads to its treatment as waste. Flax shives have recently begun to be used as fillings in composite materials [27]. The search for a way to sustainably use such biomass is still ongoing.

Taking the above into account, pyrolysis products from waste biomass (biochar) [26 [28] [29] and the so-called green synthesis products may be an interesting alternative to classic carbon additives [30]. The use of biochar as an additive to lubricants and greases is consistent with the principles of "green tribology' [31] and circular economy [32 [33]. Replacing typical carbon additives with materials derived from biomass, especially from lignocellulosics precursors, would solve at least some of the environmental problems [34–37].

This makes it possible to replace natural graphite with an environmentally neutral product: biochar derived from agricultural waste. It has been proven that lignocellulosic-based biochar is a sustainable material of very good lubrication performance on working steel surfaces, due to the affinity of biochar to steel and the formation of thin biocarbon layers on the friction surfaces [38]. At the same time, it would contribute to the sustainable use of fossil raw materials. Due to the increasing market demand for graphite, this fossil resource depletion will have a significantly greater negative impact on the natural environment, additionally increasing the price pressure on the final product. Moreover, natural graphite is classified as a strategic and critical raw material (CRM) of high importance to the EU economy and of high risk associated with its supply [39]. This is the result of a wide range of applications (in the modern technology industry and in the production of infrastructure elements necessary for the energy transformation, among other things) and an increasingly lower supply, dominated by one country (China) [40].

The paper presents the results of an analysis of two types of biochar (from waste biomass of wheat and flax) used as a lubricity additive for greases based on mineral oils. Based on the literature, it is known that the results of tribological tests show considerable unplanned and uncontrollable variations (resulting from, among others, tribotester configuration, test methodology, used materials, and misinterpretation), which often leads to unsupported conclusions or logical inconsistencies [14]. Therefore, to ensure high quality of research, it is important not only to perform a statistical analysis of the results obtained in many repetitions [41], but also to precisely examine the working surfaces in terms of tribofilm formation.

The aim of this work was to investigate the effect of biochar additives on the lubricating properties of the tested compositions and to identify the interaction of the biochar grease components with the sliding surface of steel pairs during friction in linear contact (block-on-ring).

A novelty of this research is primarily the recognition of the possibility of effectively replacing a critical raw material (graphite), used as an antiwear additive to greases, with biochar based on waste biomass from crops very popular in Europe. The added value of this research is the idea for ecological management of surplus straw and shives in accordance with the 6R principles, in particular: reduce (an attempt to eliminate the presence of graphite additive and replace it with biochar) and reuse (reuse of waste plant biomass).

2. Experimental details

2.1. Materials

Two types of biochar obtained as a result of pyrolysis of waste plant

biomass were tested: wheat straw (S) and flax shives (L). The biochar was used as an antiwear additive to model grease based on mineral oil and lithium soap. Lithium grease was chosen as the model grease because of its widespread use. It is the most popularly used grease in the world (approximately 75 % of lubrication applications in all industries). In previous works [42], greases enriched with these additives showed good antiwear and anti-seize properties. The tribological characteristics of the greases' compositions were determined using a four-ball tester in accordance with the requirements of the subject standards. The impact of biochar greases on friction surfaces has not been studied in previous works.

2.2. Biomass pyrolysis

Two types of biochar obtained by pyrolysis of waste plant biomass (wheat straw and flax shives) from typical seasonal agricultural crops in Poland were tested. The shredded waste was thoroughly mixed to obtain representative material for testing. The biochar additives were obtained through pyrolysis of biomass at 700 °C (heating rate: 10 °C/min; CO_2 protective gas flow: 5 dm^3/min) in a Czylok FCF-V12RM laboratory furnace. The parameters of pyrolysis were based on previous studies that indicated an advanced destruction of cellulose at 700 °C [43]. Once the final temperature was reached, the biochar samples were stabilised for 15 min and then allowed to cool down spontaneously (to room temperature) in a CO_2 atmosphere. The total weight reduction of biomass during pyrolysis was up to 70 %. The biochar produced was mechanically ground and sieved. The diameter of the grains of the resulting powder ranged between 80 μm and 150 μm (measured by a vibrating sieve machine Retsch AS 200). The elemental composition of biochar from wheat straw and flax shives, determined by the EDS, was presented in the previous work: in particular, the carbon content was in the range of 53–59 % [43 [44].

2.3. The preparation of biochar grease

The model grease (hereinafter the MG) was composed on the basis of highly refined paraffin oil and thickener – lithium stearate. The only additive was biochar powder (wheat- or flax-based) in the amount: 3 % or 5 % of the weight of the model grease. The model grease was homogenised by means of a high pressure apparatus. The biochar powder was dispersed in a solid form in the grease compositions during slow mixing.

The symbols and characteristics of the grease samples tested are presented in Table 1.

All the grease samples (before and after the addition of biochar) had an NLGI grade of 2. The consistency of the grease was measured with a laser penetrometer.

2.4. Tribological measurements

The tribological tests of the biochar greases were carried out using a block-on-ring tribometer according to the ASTM G77-17 standard (Standard Test Method for Ranking Resistance of Materials to Sliding Wear Using Block-on-Ring Wear Test). The linear contact was induced by the surface of the block (16 mm × 6 mm) pressed against the rotating ring (Fig. 1). All tests were performed under boundary lubrication conditions, according to the parameters given in Table 2. Boundary lubrication was the prevailing regime because under high load conditions metal-to-metal contact occurs between two sliding surfaces (with a very thin film of grease). A block-on-ring tribometer simulates real operating conditions (typical for graphite grease applications) and enables wear testing.

Table 1
The identification and composition of the tested grease samples.

Sample symbol	Composition of the grease samples
MG	Model grease
MG+3°%S	Model grease +3 wt% wheat biochar powder
MG+5°%S	Model grease +5 wt% wheat biochar powder
MG+3°%L	Model grease +3 wt% flax biochar powder
MG+5°%L	Model grease +5 wt% flax biochar powder

Fig. 1. Block-on-ring friction pair.

The friction pair was lubricated with approximately 0.04 g of the tested greases, applied once before the start of the test. The duration of the test was approximately 56 min. During the tribological tests, force values were automatically recorded at 8 s intervals. Coefficient of friction was then calculated on the basis of the value of the friction force. The average coefficient of friction was determined from three results. The measurement results were averaged using an Excel spreadsheet. The average friction coefficients corresponding to the measurement points were used to present the dependence of the friction coefficient on sliding distance.

The blocks were mechanically polished. Prior to use, the standard test elements were ultrasonically cleaned in n-hexane for 15 min each. They were finally dried in a vacuum oven at ambient temperature for 10 min and stored in a dry-box until use. After each tribological test, the blocks were also ultrasonically cleaned in n-hexane for 15 min.

2.5. The description of biomass and biochar

2.5.1. Fourier transform infrared spectrospectrometry

The biomass and biochar IR spectra were recorded using a Jasco FTIR

Table 2
Tribological test conditions.

Parameter	Value
contact geometry	block sliding on rotating ring
block and ring material	100 Cr6 steel
surface roughness	0.32 μm
hardness	65 HRC
ring dimensions	outer diameter 35 mm
block dimensions	16 × 10 × 6 mm
load	300 N
sliding speed	0.3 m/s
sliding distance	1000 m
temperature	20±2°C (ambient)
humidity	52 ± 3 % (ambient)

6200 spectrometer in a reflectance mode, with a diamond ATR detector attached. The measurement parameters were as follows: spectral range: 4000–650 cm^{-1}; spectral resolution 4 cm^{-1}; number of scans: 30. To define the exact position of some overlapping bands, deconvolution was performed using the Gauss function with full width at half maximum (FWHM) of 30, with the use of the curve fitting option available in *Spectra Manager ver. 2.*

2.5.2. Raman spectroscopy

Raman spectra were recorded with a Jasco NRS-5100 spectrometer, using a 50*x* LWD lens and green laser excitation at 532 nm for an exposure time of 60 s. The spectra were recorded for a range between 3700 and 100 cm^{-1}, with a resolution of 3.2 cm^{-1}. A biochar sample was evenly distributed on a microscope slide as a compact layer. To ensure the reliability of the results, spectra for each sample were recorded three times from different locations using the options of the *Spectra Manager* software. The intensity of the D and G bands was then determined on the basis of the peak area between 1250 ÷ 1430 cm^{-1} and 1500 ÷ 1650 cm^{-1}, respectively, corresponding to the disorder/order of the graphite-like structure. The obtained values were used to calculate the intensity ratio of D to G peak (I_D/I_G) and the arithmetic mean of the three measurements was given as a result. More information on the evaluation of biochar by Raman spectroscopy is given in the previous study [45].

2.6. The description of the worn surface

2.6.1. Profilometry

The worn surface (wear track on the block) was examined using a Talysurf CCI-Lite Non-contact 3D Profiler. The measurements were taken for each sample in accordance with the adopted procedure. Three measurement locations were indicated for each wear track: two shifted 10 % of the sample width from the edge of the specimen and one shifted it in the middle of the wear track. Topography maps of each of these locations were made, and then a cross-section in the middle of each map was drawn. On the cross-sectional profiles obtained, the area between the reference line and the wear track curve was integrated using the *TalyMap* software. The results obtained for different measurement locations were averaged. The volume wear was calculated as a multiplication of the measured area (average wear track cross-sectional area) shown in Fig. 2 and the length of the block.

Three blocks, tribologically tested for each grease, were measured profilometrically, which determined the volumetric wear. The arithmetic mean and standard deviation were calculated from the three results. The volumetric wear of the counter-sample could not be measured because the interaction of the roller with the block in the friction pair (Fig. 1) caused wear of the roller over its entire width.

2.6.2. Scanning electron microscopy/energy dispersion spectroscopy

The worn surface (wear track on the block) was analysed using a Hitachi SU-70 field-emission Scanning Electron Microscope (SEM), integrated with a Thermo Scientific Energy Dispersive Spectrometer (EDS). It was operated under a vacuum of 10^{-8} Pa. The spectra were acquired at an accelerating voltage of 15 kV and a take-off angle of 30.6° using a secondary electron detector. The elemental composition of the surface was determined as the arithmetic mean of the results recorded at three randomly selected points of the initial surface of the steel or the wears track on the steel.

2.6.3. X-ray photoelectron spectroscopy

X-ray photoemission (XPS) studies were performed with a PHI5700/660 Physical Electronics spectrometer. The XPS measurements were obtained using a monochromatic x-ray source Alk_α ($h\nu$ = 1486.6 eV). The survey spectra were obtained at a wide range of binding energy. The core lines of C1s, O1s, Fe2p, and Fe3p + Li1s region were recorded at high resolution parameters of energy and pass energy of 23.5 eV. The background of the core lines was subtracted by the Shirley method. The analysis of the shape of the photoemission lines and the calculation of the atomic concentrations were performed using *MultiPak ver. 9.8.0.19* (Ulvac-phi Incorporation).

3. Results and discussion

3.1. Analysis of the microstructure of biomass and biochar additives

3.1.1. FTIR spectrospectrometry

Spectral analysis was used to study the presence of functional groups in the lignocellulose-based biochar. The FTIR test results for the wheat-based biochar and the initial biomass are presented in Fig. 3.

The comparative analysis of the spectra obtained clearly indicates that bands observed in the initial biomass (Fig. 3a) corresponded to vibrations of the O-H bond in the hydroxyl group (~3335 cm^{-1}), and that C-O-C groups in the glycosidic bond (~1034 cm^{-1}), were not present in the biochar spectrum (Fig. 3b). This demonstrates the destruction of these structures during high-temperature pyrolysis. However, other bands indicating the presence of conjugated C=C bonds in its structure are observed in the biochar spectrum, as evidenced by the spectral band at a wavenumber of ~1620 cm^{-1}. Additionally, other overlapping bands are also observed in the range between 1600 and 1700 cm^{-1}. The

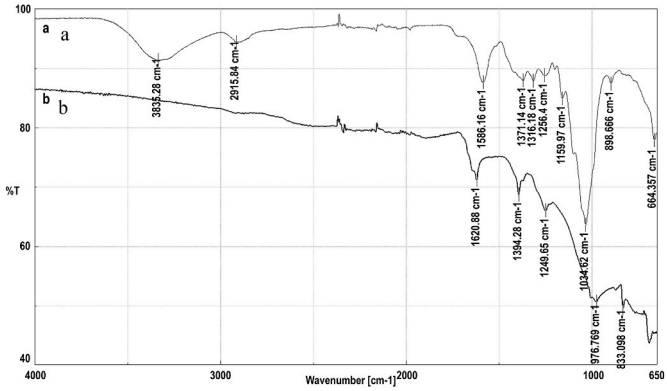

Fig. 3. Comparison of FTIR spectra for: wheat biomass (a) and wheat-based biochar (b).

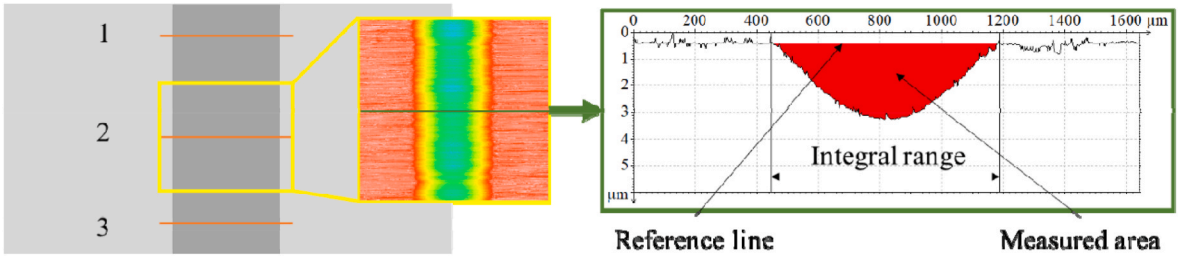

Fig. 2. The method of profilometry cross-sectional area measurement.

deconvolution enabled the determination of the exact position of individual signals (Fig. 4).

The presence of signals at ~1668 cm^{-1} and ~1647 cm^{-1} wavenumbers (Fig. 4b) indicates the presence of conjugated C=O and C=C groups in the biochar structure. The analysis of the FTIR spectra indicates that, during pyrolysis, the wheat straw biomass undergoes a structural conversion, resulting in the creation of cyclic rings containing conjugated C=C bonds and organooxygen compounds characteristic of ketones. Similar observations were made by M.R. Axet et al. [46] who reviewed various publications on the FTIR spectra of carbon materials.

The pyrolysis of flax biomass leads to the destruction of all organic groups, i.e. glycosidic, hydroxyl, and hydrocarbon bonds (Fig. 5a), as evidenced by the lack of corresponding signals in the biochar FTIR spectrum (Fig. 5b) at wavenumbers: 1031 cm^{-1}, 3326 cm^{-1}, 2918 cm^{-1}, and 2851 cm^{-1}.

Low-intensity signals are observed in the FTIR spectrum of flax shive-based biochar (Fig. 5b), which may be related to the presence of oxygen functional groups in the biochar structure. However, they are not as clearly visible as in the case of wheat-based biochar (Fig. 5b).

3.1.2. Raman spectroscopy

Biochar additives have been tested for their use as a substitute for natural graphite in plastic greases. Therefore, it is important that these are materials with controlled structural features. The I_D/I_G ratio, determined using Raman spectroscopy, allows for the assessment of the content of ordered structures (graphite-like structures) in biochar. The lower this ratio, the higher the content of graphite-like structures in the additives. The results obtained for wheat- and flax-based biochar are shown in Fig. 6.

The following bands are present in the spectra presented in Fig. 6,: 1596 cm^{-1} – corresponding to ordered graphite-like structures (G-band) and 1345 cm^{-1} – corresponding to amorphous carbon structures (D-band) [47,48]. The I_D/I_G ratio for the flax-based biochar is 0.33, while for the wheat-based biochar it is 0.44. This means that the flax-based biochar has a more ordered graphite-like structure than the wheat-based biochar. Therefore, it can be assumed that the chemical structure of both biochar types studied, used as lubricating additives, will, to varying degrees, affect the interaction between the grease and the sliding surface of a tribosystem.

3.2. Analysis of the antiwear performance of biochar additives

The relationship between the coefficient of friction and the sliding distance during friction tests with the greases tested (Fig. 7) was analysed. The measurements indicate that there are fluctuations in the friction coefficient value in the initial phase of the tribotest. This happens as a result of the friction pair lapping. After this stage, friction conditions stabilise. Based on the recorded curves, it can be concluded

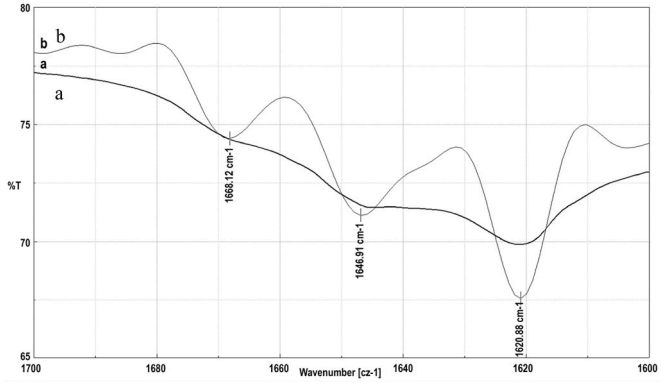

Fig. 4. Comparison of FTIR spectra (in the range 1700–1600 cm^{-1}) of wheat-based biochar: before (a) and after deconvolution (b).

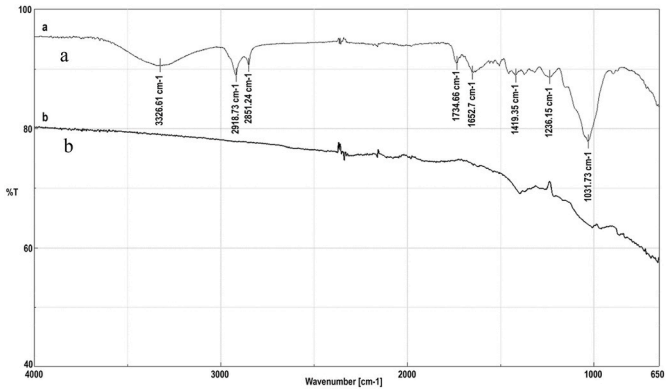

Fig. 5. Comparison of FTIR spectra of: flax biomass (a) and flax-based biochar (b).

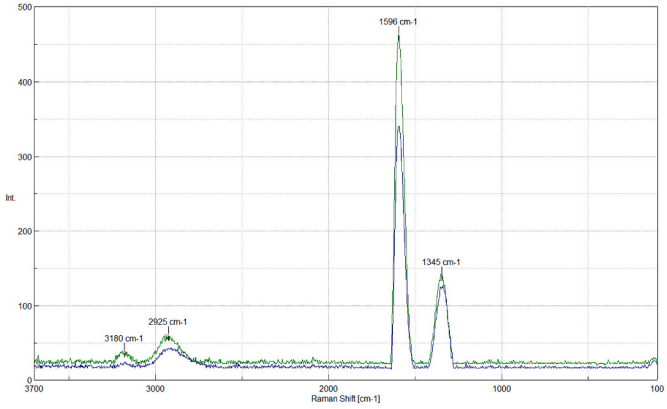

Fig. 6. Raman spectra of: flax-based biochar (green spectrum) and wheat-based biochar (blue spectrum). (For interpretation of the references to colour in this figure legend, the reader is referred to the Web version of this article.)

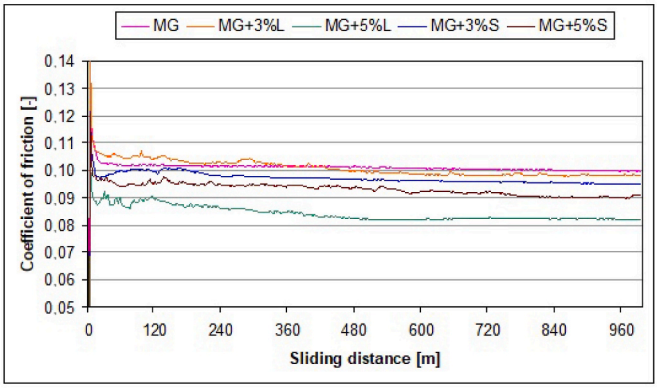

Fig. 7. Dependence of the average coefficient of friction on the sliding distance during friction tests using the plastic greases.

that the coefficients of friction during tests with the plastic greases studied range between 0.08 and 0.11.

The analysis of the results shows that, compared to the model grease (MG), the biochar in other greases reduces friction resistance The recorded curves for the greases with biochar additives mostly run below the curve recorded during tests involving the MG. The deviation is observed only in the initial phase of the curve characteristic of the MG+3°%L grease. Additionally, increasing the content of biochar in the grease causes a significant decline in the coefficient of friction. The

biochar additives to the model grease are found to reduce the coefficient of friction. Greases containing 3 wt% of biochar have recorded curves comparable to the MG model grease (Fig. 7). On the other hand, the curves recorded during tests with greases containing 5wt % of biochar indicate the stabilisation of the operating conditions after a longer distance than in the case of greases containing 3wt % of a biochar additive: in the case of MG+5 %L – after about 480 m, and of MG+5 %S – after about 800 m. This may be due to the microstructure of biochar additives, particularly the different contents of ordered/disordered graphite-like structures. Lubricants containing biochar additives with a disordered structure cause large fluctuations of the friction coefficient. This can produce different volumetric wear of the tribosystem elements. Out of the greases studied, MG+5 %L had the best tribological properties, and the recorded values of the coefficient of friction ranged between 0.08 and 0.09.

After the friction tests, block surface profilometry was carried out to analyse the volumetric wear (Fig. 8).

The application of MG+5 %S (Fig. 8c) during tribological tests reduced the volumetric wear of the block by about 21 % compared to the wear of the tribosystem lubricated with the MG (Fig. 8a). In contrast, the use of MG+5 %L under analogous conditions (Fig. 8e) reduced the tribosystem wear by about 24 % compared to the MG. It was also found that a higher biochar content (5 wt%) improved greases antiwear performance. Other published studies have shown that increasing the amount of carbon additive with an ordered structure (graphene) in the composition improves the antiwear properties of lubricant [49]. The observed effect of biochar grease on the wear of tribosystem elements is probably related to the microstructure of biochar additives. Ordered graphite-like structures may play a more important role in the antiwear performance of biochar additives than oxygen functional groups do. This may be due to the fact that the hexagonal honeycomb lattice of graphite can facilitate the transfer of grease in a tribosystem.

3.3. Analysis of the chemical structure of wear track on the block surface

Wear tracks on the surface of blocks were analysed using EDS, which allowed for the determination of elemental composition. Some examples of EDS spectra recorded in the wear track after friction between tribosystem elements lubricated with the model grease and others lubricated with biochar-enriched grease are presented in Fig. 9.

The EDS results of all blocks indicate that the presence of the main elements of steel, i.e. iron, manganese, silicon, chromium, and carbon, is observed in the wear tracks after testing with the plastic greases. Additionally, some oxygen signals were recorded, which may indicate the formation of an oxide layer, or a layer composed of organic compounds contained in the grease. It should be noted that the oxygen signal was present in the wear track after tests involving the model grease as well as the biochar-enriched greases (Fig. 9).

XPS tests were performed to better illustrate the chemical structure of the surface after friction. XPS spectra were recorded inside and outside the wear track visible in the SEM image (Fig. 10).

The surfaces of wear tracks lubricated with MG and MG+3 %L greases were analysed in detail. The results of deconvolution of carbon, oxygen and iron bands are shown in Fig. 11.

Based on the spectra presented in Fig. 11, no signals corresponding to the products of tribochemical conversion of grease components were found. In each spectrum, O1s signals at 530 eV (Fig. 11a) and Fe3p at 55.3 eV (Fig. 11c), corresponding to Fe_3O_4, were identified on the surface of the friction track. These bands were identified by comparison with the XPS spectrum of magnetite, used as a standard. In addition, other signals proving the presence of grease residue were identified. In particular, these were the O1s signals at the binding energy of 533.1 eV (Fig. 11a) and C1s at 289 eV (Fig. 11b), which are characteristic of the C=O group in lithium stearate, and the Li1s band at 52.6 eV (Fig. 11c), corresponding to the –O-Li structure in the thickener. Literature reports indicate that Li1s photoelectron signals are identified in the range from 52.3 to 54 eV, depending on the chemical composition of structures containing lithium [50]. The main C1s photoelectron signal at 285.5 eV was related to the presence of C-C structures present in the lubricant components. Moreover, in the spectrum recorded on the lubricated surface of MG+3 %L, the C1s photoelectron band was identified at 262.2 eV (Fig. 11b), probably characteristic of biochar [51].

The location of the C1s, O1s and Fe3p + Li1s photoelectron bands recorded inside the wear track and outside, where the lubricant interacted with the steel surface only statically, was compared (Fig. 12).

The addition of biochar to the lubricant reduces friction, but no differences were found in the position of the photoelectron bands on the wear track and outside it. Therefore, under friction conditions, boundary layers with products of tribochemical transformations of lubricant components are not formed. Similar observations were made by R. Yu et al. [7], who recently investigated the possibility of zinc dialkyldithiophosphate (ZDDP) film formation in rolling/sliding contacts lubricated with lithium-based grease using XPS. They found that the deposited thickener layer, although significantly reducing friction, hinders the formation of ZDDP tribofilms, in contrast to oil lubrication.

The influence of ordered graphite structures in grease reduces friction – this has been confirmed in the literature. This effect has been associated with the interlayer sliding of nano-graphite [52].

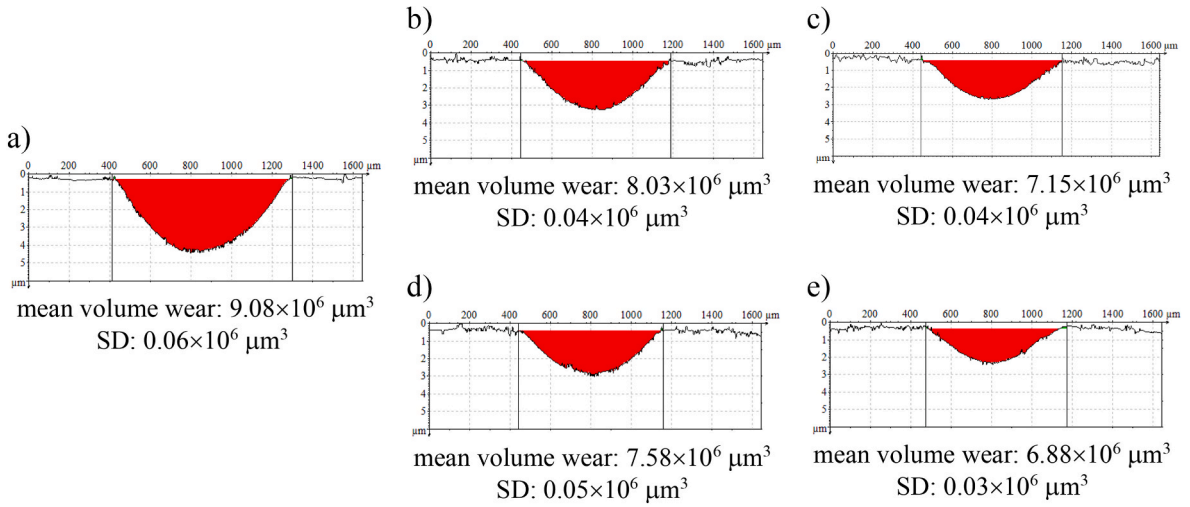

Fig. 8. Profiles and volume wear of the block, after friction, lubricated with: MG model grease (a); MG+3°%S (b) and MG+5°%S (c); MG+3°%L (d) and MG+5°% L (e).

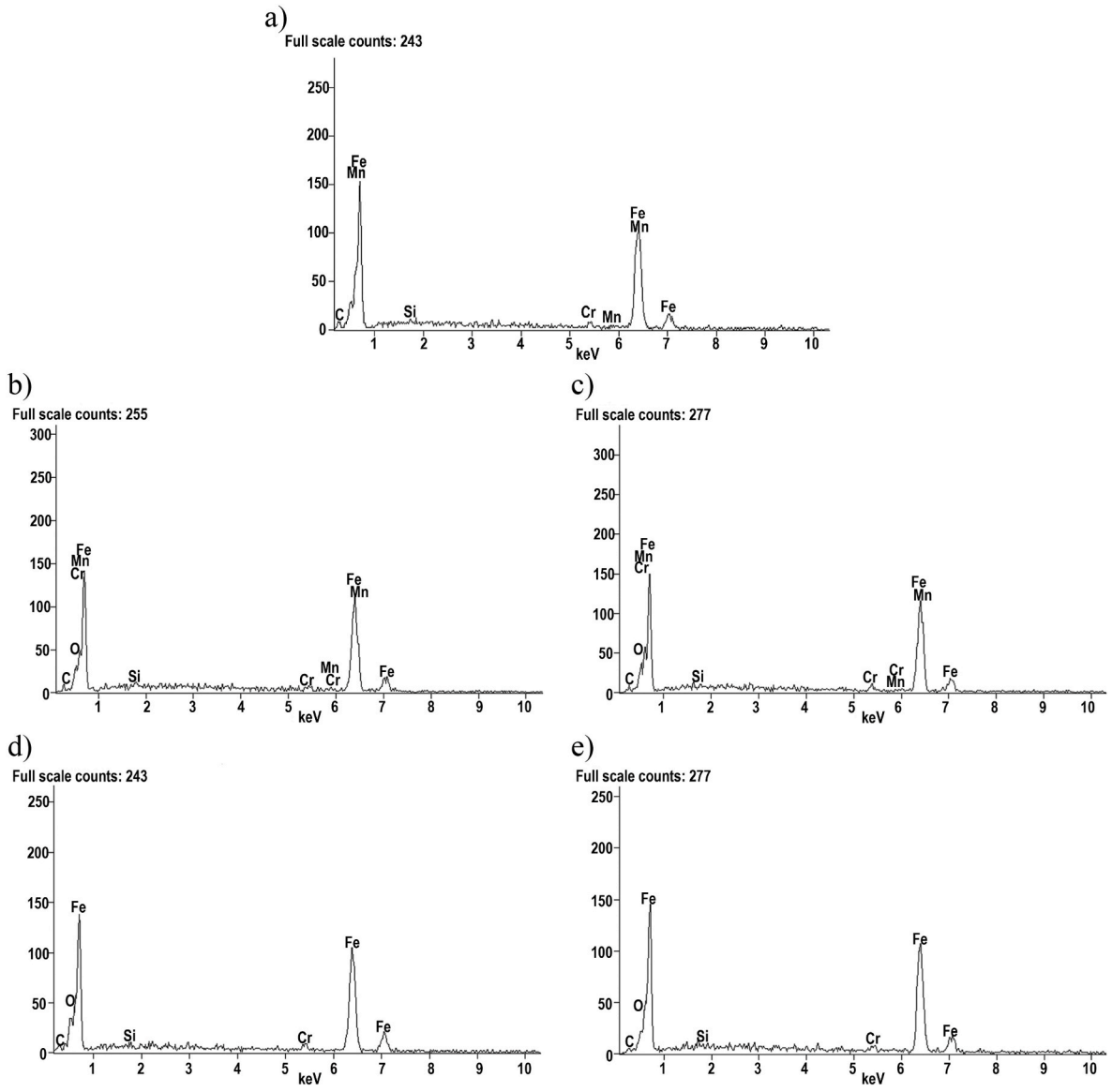

Fig. 9. EDS spectrum recorded in the wear track, after friction, lubricated with: model grease MG (a), MG+3 %S grease (b), MG+5 %S grease (c), MG+3 %L grease (d), MG+5 %L grease (e).

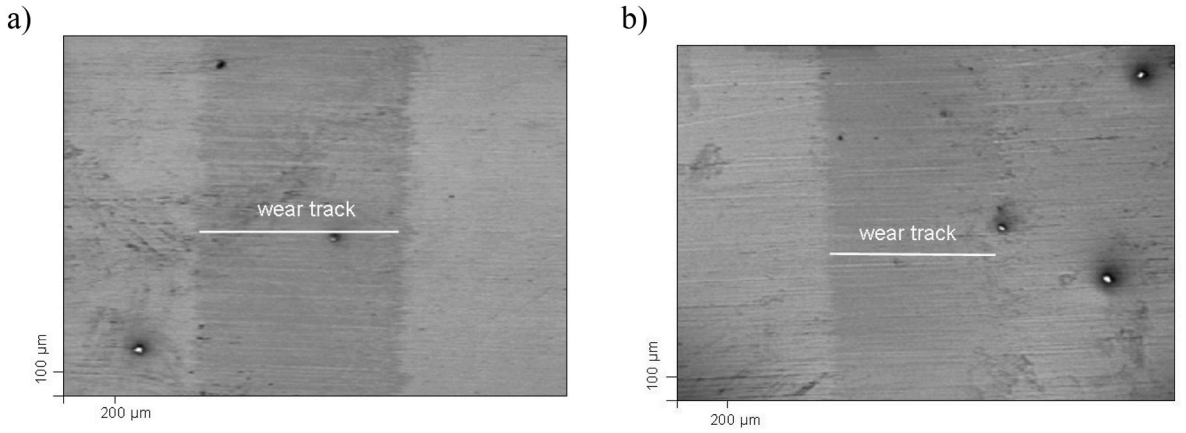

Fig. 10. SEM images of the wear tracks lubricated with: MG (a) and MG+3 %L grease (b).

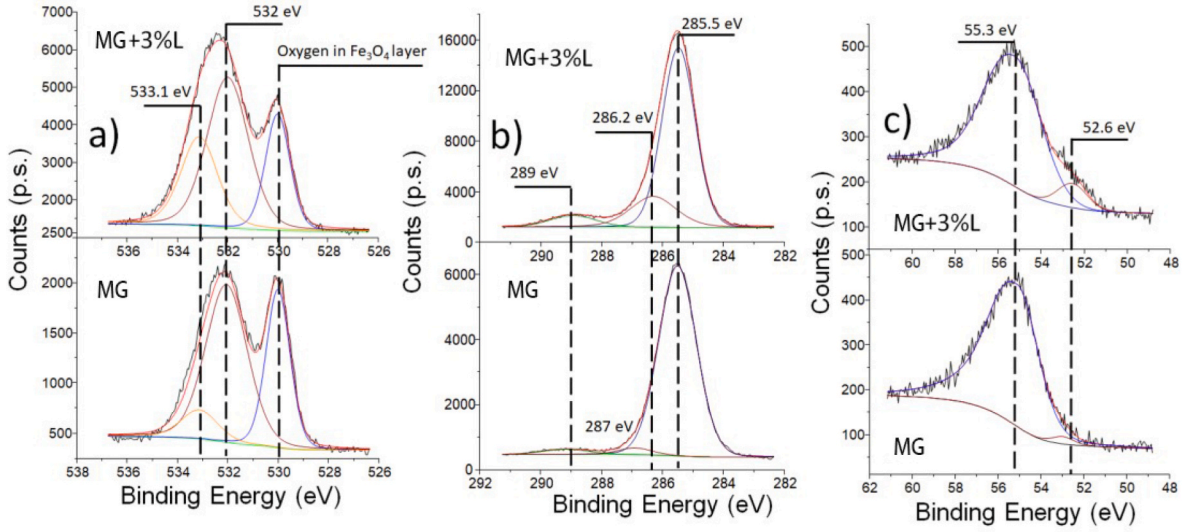

Fig. 11. Photoelectron bands O1s (a), C1s (b), and Fe3p + Li1s (c), obtained from the wear track after testing with the MG and MG+3 %L greases.

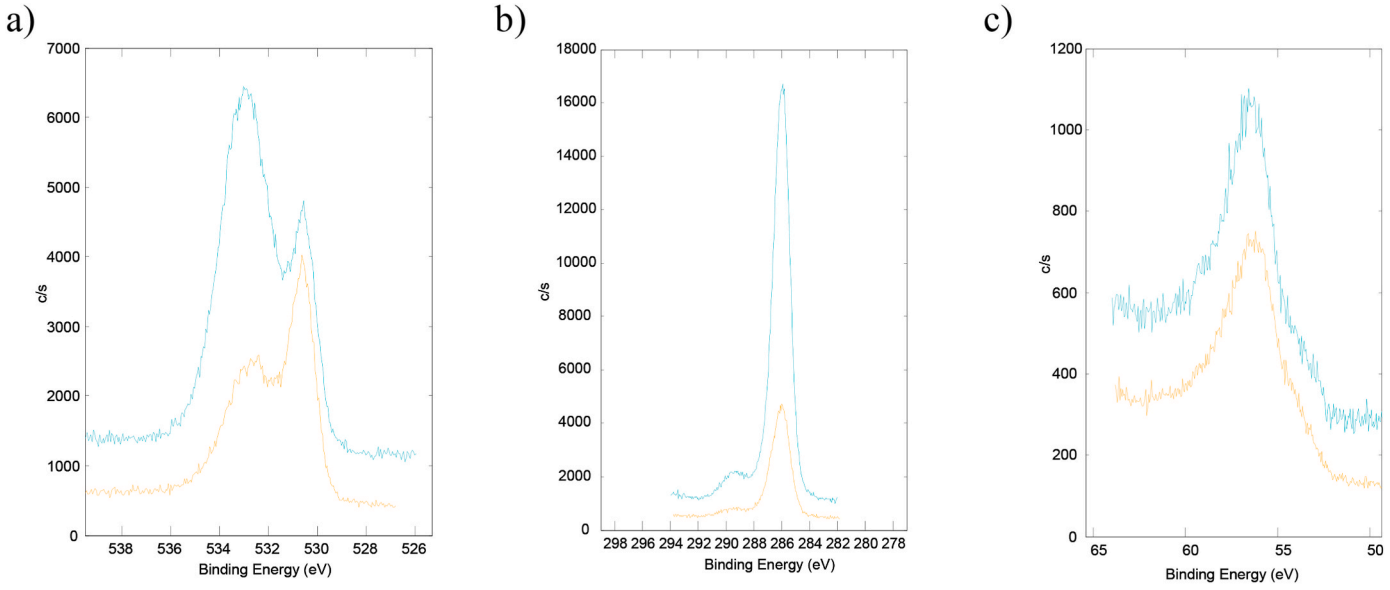

Fig. 12. Comparison of the locations of O1s (a), C1s (b), and Fe3p + Li1s (c) photoelectron bands recorded in the wear track (blue line) and outside the wear track (orange line) after testing with MG+3 %L grease. (For interpretation of the references to colour in this figure legend, the reader is referred to the Web version of this article.)

4. Conclusion

In this work, two types of biochar were produced which differed in the content of ordered graphite structures and the presence of organo-oxygen functional groups. Based on FTIR and Raman spectra, it was found that wheat-based biochar was characterised by a less ordered graphitic structure, but contained oxygen groups (including ketone groups). However, flax-based biochar was characterised by a more ordered graphite microstructure, but did not have organooxygen groups. Both types of biochar were used as additives to plastic greases. The novelty of this work is the investigation of the possibilities of effectively replacing the critical raw material (graphite) used as an antiwear additive to greases with biochar derived from agricultural waste and to study the effect of biochar on the friction surface. The conducted tests confirmed that the addition of biochar reduces the average coefficient of friction in the block-on-ring tribosystem made of bearing steel compared to the model grease. On the other hand, the volumetric wear of tribosystem elements depends on the content of biochar in the grease. The lower biochar content (in the presented tests: 3 wt%), compared to the model grease, reduces the wear of tribosystem elements regardless of the chemical structure of the biochar added. On the contrary, the impact of higher biochar content (i.e. 5 wt%) on the wear of tribosystem elements depends on the chemical structure of the biochar additive. The highest reduction in the wear of tribosystem elements is observed in the case of flax-based biochar, which has a higher ratio of ordered graphite-like structure (known as the I_D/I_G ratio) than wheat-based biochar. The I_D/I_G ratio for flax-based biochar is 0.33, while for wheat-based biochar it is 0.44. The volumetric wear of the block lubricated with MG+5 %L grease was 24 % lower than was carried the wear of the block lubricated with the model grease. XPS analyzes did not show any significant differences in the position of the spectral bands recorded in the wear track after tests with the base grease and biochar grease. Therefore, during friction under test conditions, there were no tribochemical processes changing the chemical structure of the grease components in the wear

track. The decisive factor in this case is the presence of ordered graphite-like structures in the biochar, which facilitate the interaction of the grease under frictional conditions, rather than the formation of boundary layers (including grease components) that chemically bind to the tribosystem material. The ordered graphite phase in biochar additives affects the coefficient of friction and volumetric wear of the tribosystem material – the higher the content of biochar additive with the ordered graphite-like structure, the higher the antiwear performance of the grease. These conclusions require further verification in laboratory tests. Further research will allow to determine the mechanism of boundary layer formation and arrive at conclusions to be presented in a subsequent paper.

CRediT authorship contribution statement

Jarosław Molenda: Writing – review & editing, Writing – original draft, Validation, Methodology, Investigation, Funding acquisition, Formal analysis, Conceptualization. **Monika Makowska:** Writing – review & editing, Visualization, Validation. **Jerzy Kubacki:** Writing – review & editing, Writing – original draft, Visualization, Investigation. **Marcin Sikora:** Writing – original draft, Investigation. **Maciej Łuszcz:** Writing – original draft, Investigation. **Edyta Osuch-Słomka:** Investigation.

Funding

This study was funded under a research project. The *Use of carbonisate from waste lignocellulosic biomass as a substitute for non-renewable raw materials for the production of innovative biochar greases* project is carried out within the Proof of Concept programme of the Foundation for Polish Science co-financed by the European Union under the European Funds for Smart Economy 2021–2027 (FENG).

Declaration of competing interest

The authors declare that they have no known competing financial interests or personal relationships that could have appeared to influence the work reported in this paper.

Data availability

Data will be made available on request.

References

[1] J. Wang, X. Guo, Y. He, M. Jiang, K. Gu, Tribological characteristics of graphene as grease additive under different contact forms, Tribol. Int. 127 (2018) 457–469, https://doi.org/10.1016/j.triboint.2018.06.026.
[2] K. Holmberg, A. Erdemir, Influence of tribology on global energy consumption, costs and emissions, Friction 5 (3) (2017) 263–284, https://doi.org/10.1007/s40544-017-0183-5.
[3] W. Huai, Ch Zhang, S. Wen, Graphite-based solid lubricant for high-temperature lubrication, Friction 9 (2021) 1660–1672, https://doi.org/10.1007/s40544-020-0456-2.
[4] D.A.Y. Al-Saadi, V.F. Pershin, B.N. Salimov, S.A. Montaev, Modification of graphite greases graphene nanostructures, J. Frict. Wear 38 (5) (2017) 355–358, https://doi.org/10.3103/S1068366617050026.
[5] A. Mura, F. Cura, F. Adamo, Evaluation of graphene grease compound as lubricant for spline couplings, Tribol. Int. 117 (2018) 162–167, https://doi.org/10.1016/j.triboint.2017.08.027.
[6] N. Kumar, V. Saini, J. Bijwe, Tribological investigations of nano and micro-sized graphite particles as an additive in lithium-based grease, Tribol. Lett. 68 (2020) 124, https://doi.org/10.1007/s11249-020-01362-1.
[7] R. Yu, H. Liu, Q. Sun, W. Lou, S. Zhang, X. Wang, Y. Zhao, Experimental study on ZDDP tribofilm formation in grease lubricated rolling/sliding contacts, Tribol. Int. 206 (2025) 110594, https://doi.org/10.1016/j.triboint.2025.110594.
[8] E. Larsson, R. Westbroek, J. Leckner, S. Jacobson, A.K. Rudolphi, Grease-lubricated tribological contacts – influence of graphite, graphene oxide and reduced graphene oxide as lubricating additives in lithium complex (LiX) - and polypropylene (PP) -thickened greases, Wear 486–487 (2021) 204107, https://doi.org/10.1016/j.wear.2021.204107.
[9] Z. Li, Q. He, S. Du, Y. Zhang, Effect of few layer graphene additive on the tribological properties of lithium grease, Lubr. Sci. 32 (2020) 333–343, https://doi.org/10.1002/ls.1506.
[10] D. Berman, A. Erdemir, A.V. Sumant, Graphene: a new emerging lubricant, Mater. Today 17 (2014) 31–42, https://doi.org/10.1016/j.mattod.2013.12.003.
[11] N. Nyholm, N. Espallargas, Functionalized carbon nanostructures as lubricant additives – a review, Carbon 201 (2023) 1200–1228, https://doi.org/10.1016/j.carbon.2022.10.035.
[12] A. Erdemir, G. Ramirez, O.L. Eryilmaz, B. Narayanan, Y. Liao, G. Kamath, S.K.R. S. Sankaranarayanan, Carbon-based tribofilms from lubricating oils, Nature 536 (2016) 67–71, https://doi.org/10.1038/nature18948.
[13] E. Stefan-Henningsen, N. Roberts, A. Kiani, Enhancing tribological performance: a comprehensive review of graphene-based additives in lubricating greases, RINENG 25 (2025) 104551, https://doi.org/10.1016/j.rineng.2025.104551.
[14] N.A. Ismail, N.W.M. Zulkifli, Z.Z. Chowdhury, M.R. Johan, Functionalization of graphene-based materials: effective approach for enhancement of tribological performance as lubricant additives, Diam. Relat. Mater. 115 (2021) 108357.
[15] R. Arvidsson, M. Boholm, M. Johansson, M.L. Montoya, *Just carbon*: ideas about graphene risks by graphene researchers and innovation advisors, Nanoethics 12 (2018) 199–210, https://doi.org/10.1007/s11569-018-0324-y.
[16] L. Ou, B. Song, H. Liang, J. Liu, X. Feng, B. Deng, T. Sun, L. Shao, Toxicity of graphene-family nanoparticles: a general review of the origins and mechanisms, Part, Fibre Toxicol. 13 (2016) 57, https://doi.org/10.1186/s12989-016-0168-y.
[17] O. Cebadero-Domínguez, B. Ferrández-Gómez, S. Sánchez-Ballester, J. Moreno, A. Jos, A.M. Camean, *In vitro* toxicity evaluation of graphene oxide and reduced graphene oxide on Caco-2 cells, Toxicol. Rep. 9 (2022) 1130–1138, https://doi.org/10.1016/j.toxrep.2022.05.010.
[18] X. Zhang, H. Wang, Ch Ma, N. Niu, Z. Chen, S. Liu, J. Li, S. Li, Seeking value from biomass materials: preparation of coffee bean shell-derived fluorescent carbon dots *via* molecular aggregation for antioxidation and bioimaging applications, Mater. Chem. Front. 7 (2018) 1269–1275, https://doi.org/10.1039/C8QM00030A.
[19] Q. Wang, C. Li, Y. Wang, X. Que, Phytotoxicity of graphene family nanomaterials and its mechanisms: a review, Front. Chem. 7 (2019) 292, https://doi.org/10.3389/fchem.2019.00292.
[20] N. Kobayashi, H. Izumi, Y. Morimoto, Review of toxicity studies of carbon nanotubes, J. Occup. Health 59 (2017) 394–407, https://doi.org/10.1539/joh.17-0089-RA.
[21] Z. Sun, Ch Xu, Y. Peng, Y. Shi, Y. Zhang, Fretting tribological behaviors of steel wires under lubricating grease with compound additives of graphene and graphite, Wear 454–455 (2020) 203333, https://doi.org/10.1016/j.wear.2020.203333.
[22] P. Nagarem, H. Kudalb, A Taguchi approach on influence of graphite as an anti-wear additive on the performance of lithium grease, Procedia Manuf. 20 (2018) 487–492, https://doi.org/10.1016/j.promfg.2018.02.072.
[23] JRC Technical Reports, Ecolabel Criteria for Lubricants – Final Technical Report, European Union, 2018. https://ec.europa.eu/jrc.
[24] FAO – Food and Agricultural Organisation of the United Nations, Food Wastage Footprint & Climate Change, UN FAO, Rome, 2015. http://www.fao.org/3/a-bb144e.pdf. (Accessed 29 April 2025).
[25] M. Donner, A. Verniquet, J. Broeze, K. Kayser, H. Vries, Critical success and risk factors for circular business models valorising agricultural waste and by-products, Resources, Conserv. Recycl. 165 (2021) 105236, https://doi.org/10.1016/j.resconrec.2020.105236.
[26] L. Singh, V.Ch Kalia (Eds.), Waste Biomass Management – A Holistic Approach, Springer, 2017, https://doi.org/10.1007/978-3-319-49595-8.
[27] W. Ma, L. Yan, B. Kasal, Intensive exploration: the application potential of flax fibre/textiles as reinforcement in cementitious composites, J. Clean. Prod. 507 (2025) 145457, https://doi.org/10.1016/j.jclepro.2025.145457.
[28] S.K. Tiwari, M. Bystrzejewski, A. Adhikari, A. Huczko, N. Wang, Methods for the conversion of biomass waste into value-added carbon nanomaterials: recent progress and applications, PECS 92 (2022) 94–102, https://doi.org/10.1016/j.jaap.2016.04.013.
[29] S.S. Senadheera, P.A. Withana, S. You, D.C.W. Tsang, S.Y. Hwang, Y.S. Ok, Sustainable biochar: market development and commercialization to achieve ESG goals, Renew. Sustain. Energy Rev. 201 (2025) 114799, https://doi.org/10.1016/j.wasman.2025.114799.
[30] Z. Ding, F. Li, J. Wen, X. Wang, R. Sun, Gram-scale synthesis of single-crystalline graphene quantum dots derived from lignin biomass, Green Chem. 20 (2018) 1383–1390, https://doi.org/10.1039/C7GC03218H.
[31] M. Nosonovsky, B. Bhushan (Eds.), Green Tribology. Biomimetics, Energy Conservation and Sustainability, Springer, 2012, https://doi.org/10.1007/978-3-642-23681-5.
[32] F.R. Oliveira, A.K. Patel, D.P. Jaisi, S. Adhikari, H. Lu, S.K. Khanal, Environmental application of biochar: current status and perspectives, Bioresour. Technol. 246 (2017) 110–122, https://doi.org/10.1016/j.biortech.2017.08.122.
[33] Y. Zhou, S. Qin, S. Verma, T. Sar, S. Sarsaiya, B. Ravindran, T. Liu, R. Sindhu, A. K. Patel, P. Binod, S. Varjani, R.R. Singhnia, Z. Zhang, M.K. Awasthi, Production and beneficial impact of biochar for environmental application: a comprehensive review, Bioresour. Technol. 337 (2021) 125451, https://doi.org/10.1016/j.biortech.2021.125451.
[34] P. González-García, Activated carbon from lignocellulosics precursors: a review of the synthesis methods, characterization techniques and applications, Renew. Sustain. Energy Rev. 82 (2018) 1393–1414, https://doi.org/10.1016/j.rser.2017.04.117.
[35] M.A. Yahya, Z. Al-Qodah, C.W.Z. Ngah, Agricultural bio-waste materials as potential sustainable precursors used for activated carbon production: a review,

Renew. Sustain. Energy Rev. 46 (2015) 218–235, https://doi.org/10.1016/j.rser.2015.02.051.
[36] Y. Zhang, Z. Ding, M.S. Hossain, R. Maurya, Y. Yang, V. Singh, D. Kumar, E. S. Salama, X. Sun, R. Sindhu, P. Binod, Z. Zhang, M.K. Awasthi, Recent advances in lignocellulosic and algal biomass pretreatment and its biorefinery approaches for biochemicals and bioenergy conversion, Bioresour. Technol. 367 (2023) 128281, https://doi.org/10.1016/j.biortech.2022.128281.
[37] L. Zhu, H. Lei, Y. Zhang, X. Zhang, Q. Bu, Y. Wei, L. Wang, G. Yadavalli, E. Villota, A review of biochar derived from pyrolysis and its application in biofuel production, SF J. Mater. Chem. Eng. 1 (2018) 1007. https://scienceforecastoa.com.
[38] S. Mehta, P. Joshi, A. Pandey, R.N. Goswami, O.P. Sharma, O.P. Khatri, Graphitic biocarbon from agrowaste biomass: a sustainable material of excellent lubrication performance, ACS Sustainable Resource Management 2 (1) (2025). https://pubs.acs.org/doi/10.1021/acssusresmgt.4c00411?goto=supporting-info. (Accessed 5 May 2025).
[39] Critical Raw Materials: Ensuring Secure and Sustainable Supply Chains for EU's Green and Digital Future, European Commission, 2023. https://ec.europa.eu/commission/presscorner/detail/en/ip_23_1661.
[40] X. Rui, Y. Geng, X. Sun, H. Hao, S. Xiao, Dynamic material flow analysis of natural graphite in China for 2001-2018, Resour. Conserv. Recycl. 173 (2021) 105732, https://doi.org/10.1016/j.resconrec.2021.105732.
[41] M. Watson, et al., An analysis of the quality of experimental design and reliability of results in tribology research, Wear 426–427 (2019) 1712–1718, https://doi.org/10.1016/j.wear.2018.12.028.
[42] J. Molenda, Z. Pawelec, E. Pawelec, B. Kaźmierczak, The influence of biocarbon additives on grease functionality, Tribologia 2 (2020) 47–53, https://doi.org/10.5604/01.3001.0014.3739.
[43] J. Molenda J., M. Swat, E. Osuch-Słomka, Effect of thermal conditions of pyrolysis process on the quality of biochar obtained from vegetable waste, Engineering and Protection of Environment 3 (2018) 289–302, https://doi.org/10.17512/ios.2018.3.7.
[44] J. Molenda, M. Swat, M. Wolszczak, The chemical composition and microstructure of biocarbons received by pyrolysis from vegetable waste, Przemysł Chemiczny 97 (8) (2018) 1380–1386, https://doi.org/10.15199/62.2018.8.29.
[45] M. Makowska, K. Dziosa, Influence of different pyrolysis temperatures on chemical composition and graphite-like structure of biochar produced from biomass of green microalgae *Chlorella sp*, Environmental Technology & Innovation 35 (2024) 103667, https://doi.org/10.1016/j.eti.2024.103667.
[46] M.R. Axet, O. Dechy-Cabaret, J. Durand, M. Gouygou, P. Serp, Coordination chemistry on carbon surfaces, Coord. Chem. Rev. 308 (2016) 236–345, https://doi.org/10.1016/j.ccr.2015.06.005.
[47] D. Schuepfer, F. Badaczewski, J.M. Guerra-Castro, D. Hofmann, C. Heiliger, B. Smarsly, P. Klar, Assessing the structural properties of graphitic and non-graphitic carbons by Raman spectroscopy, Carbon 161 (2020) 359–372, https://doi.org/10.1016/j.carbon.2019.12.094.
[48] S.I. Moseenkov, V.L. Kuznetsov, N.A. Zolotarev, B.A. Kolesov, I.P. Prosvirin, A. V. Ishchenko, A.V. Zavorin, Investigation of amorphous carbon in nanostructured carbon materials (A comparative study by TEM, XPS, Raman Spectroscopy and XRD), Materials 16 (2023) 1112, https://doi.org/10.3390/ma16031112.
[49] J. Molenda, R. Michalczewski, The effect of graphene additive on the tribological properties of bionic lubricant compositions tested by the SRV method, Tribologia 6 (2019) 47–56, https://doi.org/10.5604/01.3001.0013.7767.
[50] I. Ismail, A. Noda, A. Nishimoto, M. Watanabe, XPS study of lithium surface after contact with lithium-salt doped polymer electrolytes, Electrochim. Acta 46 (2001) 1595–1603, https://doi.org/10.1016/S0013-4686(00)00758-1.
[51] J. Li, X. Zeng, T. Ren, E. van der Heide, The preparation of graphene oxide and its derivatives and their application in bio-tribological systems, Lubricants 2 (2014) 137–161, https://doi.org/10.3390/lubricants2030137.
[52] M. Niu, J. Qu, Tribological properties of nano-graphite as an additive in mixed oil-based titanium complex grease, RSC Adv. 8 (2018) 42133–42144, https://doi.org/10.1039/C8RA08109C.